Capacity of UWB Wireless Channel for Neural Recording Systems

Mohamad El Khaled, Hadi Bahrami, Paul Fortier, Benoit Gosselin and Leslie Ann Rusch

***Abstract*— Ultra wide-band (UWB) short-range communication systems are valuable in medical technology, particularly for implanted devices, due to their low-power consumption, low cost, small size and high data rates. Monitoring of neural responses in the brain requires high data rate if we target a system supporting a large number of sensors. In this work, we are interested in the evaluation of the capacity of the ultra wide-band (UWB) channel that we could exploit using a realistic model of the biological channel. The channel characteristics are examined under two scenarios that are related to TX antenna placements. Using optimal power spectrum allocation (OPSA) at the transmitter side, we have computed this capacity by taking into account the fading characteristics of the channel. The results show the pertinence of the optimal power spectrum allocation for this type of channel. An improvement by a factor of 2 to 3 over a uniform power spectrum allocation (UPSA) when the SNR $<$ 0 dB was obtained. When the SNR is $>$ 40 dB, both approaches give similar results. Antennas placement is examined under two scenarios having contrasting power constraints.**

I. Introduction

There is a growing interest for implantable transmitters to extract the raw electrophysiological data gathered from miniature monitoring implanted systems [1], [2]. These emerging devices are crucial components in the development of new medical applications targeted at diagnostic and treatment of neurological diseases and/or at control of prosthetic devices [3]. Such applications require a high-capacity wireless link between an implanted device and an external controller for supporting data rates that can typically reach hundreds of Mbits/s.

Ultra wide-band (UWB) signals are transmitted in the unlicensed Federal Communications Commission (FCC) approved frequency range (3.1-10.6 GHz). UWB offers several advantages over narrowband systems such as higher bit rates, low power consumption, and highly integrated systems featuring smaller antenna size [4] that are suitable for implanted short range applications. The transmission loss for the human head in the 100 MHz to 6 GHz band was found for a mm-size antenna without specific consideration of the bandwidth of the antenna or the effect of biological tissues on systems performance [5], [6]. Recently, we have introduced a methodology for designing a reliable wireless link for neural recording system using tissue modelling and designing suitable antennas for this type of applications [5], [6]. Because of the near filed communications of the antennas in neural recording, the antennas and the channel cannot be treated separately and need to be simulated holistically. Simulations were carried out with HFSS, exploiting a layered model with differing dielectric constants to capture the effect of surrounding tissues [5], [6]. The multilayer of tissues between TX and RX antennas cause small scale variations of the received signal resulting in frequency selectivity of the channel. Prior works have been published for the capacity of the indoor UWB channel for free space [7]. However the effects of biological tissues must be taken into account. The aim of our work is to study the theoretical capacity of the neural recording UWB channel considering the channel fading characteristics.

In section II, we present the dielectric tissue model used for channel modelling, and also consider channel characteristics for two scenarios for the location of the implant. Section III presents an analytical method to compute the theoretical capacity of the neural recording UWB channel taking into account frequency selectivity. In section IV, computation results are presented and analyzed. Finally, conclusions are drawn in section V.

II. Characterization of UWB channel under two scenarios

A. Multi-layer Model of Tissues

Transmission is captured by $H(\omega)$, the frequency response of the neural monitoring channel, which is given by:

$$H(\omega) = A(\omega)\, e^{j\theta(\omega)} \tag{1}$$

where $A(\omega)$ and $\theta(\omega)$ are the amplitude and phase, respectively [8]. Unlike free space communications, the multiple biological tissues in neural monitoring systems have varying conductivity and dielectric constants leading to complex RF interaction [9]. The thickness and electrical properties of each tissue layer impact the overall antenna performance.

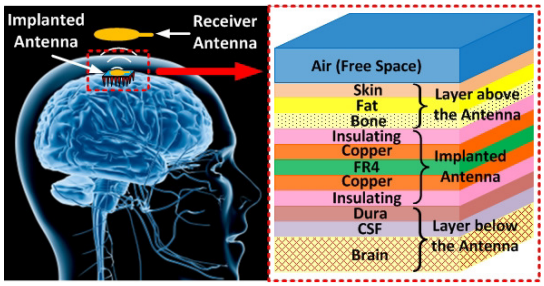

Fig. 1: Multi-layer inhomogeneous model of the head as wireless channel in HFSS.

This work was supported in part by the Natural Sciences and Engineering Research Council of Canada and by the Regroupement Stratégique en Microsystèmes du Québec. The authors are with the Dept. of Electrical and Computer Engineering, Université Laval, Québec, QC G1V 0A6, Canada. E-mail: mohamad.el-khaled.1@ulaval.ca

978-1-4244-7929-0/14/$26.00 ©2014 IEEE

Type of tissue	Best case (mm)	Worst case (mm)
Skin	0.5	1.0
Fat	0	2.0
Bone	2.0	7.0
Dura	0.5	1.0
CSF	0	2.0
Brain	40.0	40.0

TABLE I: Worst case and best case of thickness of head tissues.

In previous works [5], [6], a multilayer model of head tissue which is shown in Fig. 1 was used for modelling the wireless channel for different scenarios (Figures 2 and 3). For this modelling, we have used a commercial finite element method solver (HFSS software) to represent head tissues as a sequence of dielectric layers with defining frequency dependent dielectric properties of layers in UWB band inside the software. We model each biological tissue as a dispersive dielectric using two electrical parameters: relative permittivity and loss tangent. The frequency dependent relative permittivity and loss tangent are available in [10] for the entire UWB band. The loss tangent quantifies inherent dielectric dissipation when interacting with an electromagnetic wave. The multi-layer model includes the brain matter, the cerebrospinal fluid (CSF), the dura, bone (skull), fat, and skin. The thickness of each layer will affect antenna propagation behaviour, hence we consider two extreme cases, minimum and maximal adult tissue thicknesses, that are indicated in the Table I [9]. The worst case (i.e., leading to greatest signal attenuation) occurs with the maximum thicknesses. The antennas (TX and RX antennas) were designed by taking into account the impact of the surrounding tissues. A miniature implanted antenna surrounded by biological tissues will have a very different radiation pattern than one in free-space, hence the gain and directivity of the antennas will be affected. As the impedance of the biological tissues is very different from that of free space, careful impedance matching is required; return loss must be calculated with the impact of tissue impedance included [5], [6]. The tissue impact on antenna response will vary with position, hence antenna design and performance will differ across the two scenarios. We have designed two antennas suitable for the locations [6].

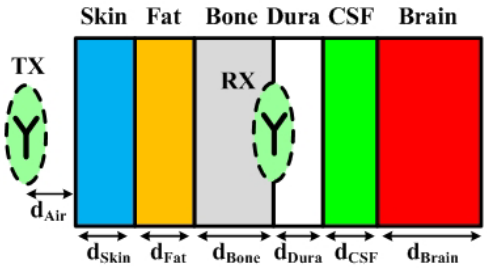

Fig. 2: Wireless channel model of scenario 1 in HFSS.

By modelling the head tissues and designing suitable implanted TX and exterior RX antennas in HFSS, we can

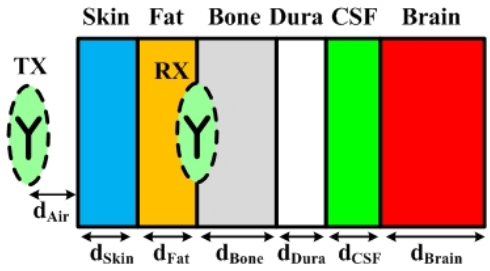

Fig. 3: Wireless channel model of scenario 2 in HFSS.

get the channel frequency response (S21). The simulation S21 results are plotted in figures 4 and 5. The figures show that the insertion loss of the channel increases with tissue thicknesses and frequency. At higher frequencies, the loss tangent of tissues increases, which causes more loss when electromagnetic waves propagate in thicker tissues. As absorption in tissues increases with frequency, analyses show that lower frequency should be exploited to improve transfer efficiency. Figures 4 and 5 depect the magnitude and the phase of the frequency response for both scenarios. In scenarion 1, the TX antenna is located between bone and dura. For Scenario 2, the TX antenna is located one layer higher between fat and bone. As we can see in Fig. 5, the phase of the channel is close to being linear. A non-ideal channel frequency response is caused by amplitude and phase distortions. As we can see from Fig. 4, most of the distortion in this application is related to the amplitude.

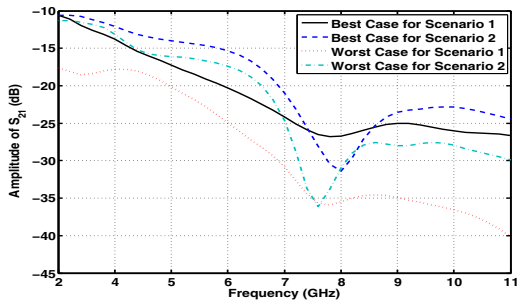

Fig. 4: Magnitude of the frequency response for both scenarios.

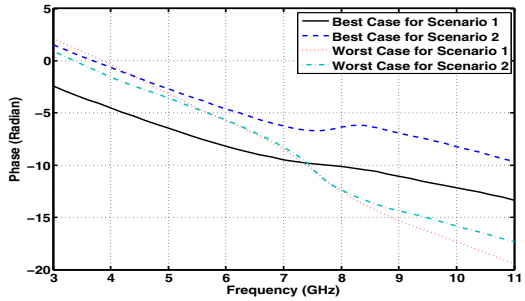

Fig. 5: Phase of the frequency response for both scenarios.

III. Capacity of the biological UWB channel

In the following, we use the approach developed by Zheng and Kaiser to compute the capacity of the channel [7]. Shannon's formula represents the classical way to compute the capacity of an AWGN channel. It is given by:

$$C = B\log_2\left[1+\rho_R\right] \tag{2}$$

where ρ_R is the signal-to-noise ration (SNR) at the receiver, given by :

$$\rho_R = |H(f)|^2\rho_T \tag{3}$$

where $H(f)$ is the frequency response of the channel and ρ_T is the SNR at the transmitter. We suppose that the transmitted signal power is limited according to

$$\int_{-\frac{B}{2}}^{\frac{B}{2}} S_X(f)df = P \tag{4}$$

where $S_X(f)$ is the PSD of the transmitted signal $X(t)$, B is the transmitted signal bandwidth and P is the maximum power available at the transmitter. In practice, UWB channel has multipath. This makes the UWB channel selective in the frequency domain. In order to compute the capacity in such cases, we must divide the channel into a multitude of narrowband frequency flat sub-channels and apply Shannon's formula on each of these sub-channels. Thus, the capacity is equivalent to:

$$C = \max_{S_X(f)} \int_{-\frac{B}{2}}^{\frac{B}{2}} \log_2\left[1+\frac{S_X(f)|H(f)|^2}{N_0}\right]df \tag{5}$$

where $S_X(f)$ subject to the constraint in (4). If the information on $H(f)$ is available at the transmitter, an optimized power distribution can be applied in order to maximize the capacity for a given transmission power. Using this method, called "waterfilling", the power spectral density $S_X(f)$ can be computed according to:

$$S_X(f) = \left[\alpha - \frac{N_0}{|H(f)|^2}\right]_+ \tag{6}$$

where $[x]_+$ is equal to x when $x \geq 0$ and 0 otherwise and α is a constant verifying the following equation:

$$\int_{f\in F_\alpha \subset [-\frac{B}{2},\,\frac{B}{2}]} \left[\alpha - \frac{N_0}{|H(f)|^2}\right] = P \tag{7}$$

where F_α is the frequency range such that $\frac{N_0}{|H(f)|^2} \leq \alpha$. The optimal solution $S_X(f)$ is what is obtained from the waterfilling algorithm.

Substituting (6) into (5) we obtain the optimal channel capacity:

$$\begin{aligned} C &= \int_{f\in F_\alpha \subset [-\frac{B}{2},\,\frac{B}{2}]} \log_2\left[1+\frac{\left(\alpha-\frac{N_0}{|H(f)|^2}\right)|H(f)|^2}{N_0}\right]df \\ &= \int_{f\in F_\alpha \subset [-\frac{B}{2},\,\frac{B}{2}]} \log_2\left[\overline{\alpha}|H(f)|^2\right]df \end{aligned} \tag{8}$$

where $\overline{\alpha} = \alpha/N_0$. If the information on $H(f)$ is not available at the transmitter, the simplest method to compute the channel capacity is to distribute uniformly the power over the signal bandwidth. Using this method the channel capacity is given by:

$$\int_{-\frac{B}{2}}^{\frac{B}{2}} \log_2\left[1+\rho_T\,|H(f)|^2\right]df \tag{9}$$

IV. Numerical results and Comparisons

A. Optimal power spectrum allocation (OPSA) vs uniform power spectrum allocation (UPSA)

Let C_{Unif} and C_{Optim} denote the capacity of the system for the UPSA and OPSA schemes, respectively. The optimal channel capacity is given by

$$C_{Optim} = \sum_{i=1}^{N} \Delta f \times \log_2\left[\overline{\alpha}|H(f_i)|^2\right] \tag{10}$$

where $f_i \in F_\alpha$, $N = 41$, corresponding to the number of sweep points and Δf is the sub-channel bandwidth and is equal to 219.5122 MHz in our case. The uniform channel capacity is given by:

$$C_{Unif} = \sum_{i=1}^{N} \Delta f \times \log_2\left[1+\rho_T\,|H(f_i)|^2\right] \tag{11}$$

In our computations, we divided the channel into several sub-channels (41 in our case, corresponding to the number of sweep points) with the bandwidth of every sub-channel equal to Δf [7]. Then, we attributed to each sub-channel a power optimizing the total capacity (waterfilling). In doing so, we considered only the sub-channels that had a ratio $\frac{1}{|H(f)|^2} < \overline{\alpha}$, where $\overline{\alpha}$ is a constant obtained from the waterfilling method.

Figures 6 and 7 show the uniform and the optimal capacities of the channel for neural recording systems, respectively for scenarios 1 and 2 and with two configuration for each scenario, best case and worst case. As expected, results prove that the uniform capacities of scenario 2 are higher than the capacities of scenario 1. This results can be explaned by the number of layers between the transmit and receive antennas; three layers in scenario 1 and two layers in scenario 2. The larger number of layers increases attenuation. Results also show, that the capacity of scenario 1 (best case) and the capacity of scenario 2 (worst case) are very similair. The thickness of head tissues for these cases are almost the same as summarized in Table I: 2.5 mm for the best case of scenario 1 and 3 mm for the worst case of scenario 2. Results prove that optimal power allocation increase the capacities of scenario 2 (best and worst cases) and the capacities of scenario 1 (best case and worst cases). On both uniform and optimal capacities, the worst case of scenario 1 has less capacity because of the thickness of head tissues; 10 mm in this case.

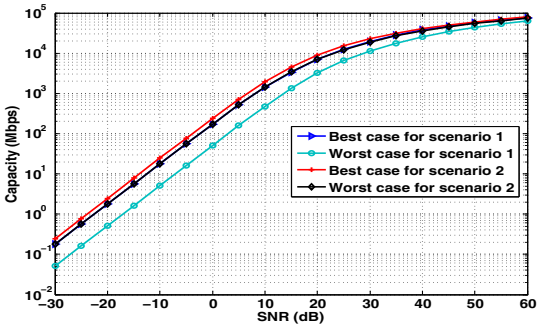

Fig. 6: Uniform capacity in Mbps.

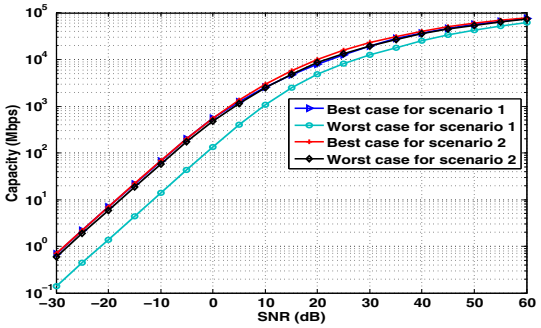

Fig. 7: Optimal capacity in Mbps.

To demonstrate the pertinence of the optimal power spectrum allocation (OPSA) scheme for the UWB channel of neural recording systems for the scenarios, we use C_{Unif}/C_{Optim} as an index for the efficiency of UPSA relative to OPSA. Fig. 8 shows the efficiency of UPSA relative to OPSA for both scenarios and demonstrates the pertinence of the OPSA method. We can see that the efficiency of UPSA is lower than 0.31 and 0.43 in the best case for scenarios 1 and 2, respectively. Also, the efficiency of UPSA is lower than 0.38 and 0.36 in the worst case for scenarios 1 and 2, respectively, when the SNR is lower than 0 dB. This says that the transmission rate can be increased more than 3.2 and 2.3 times if OPSA, instead of UPSA, is adopted in the best case for scenarios 1 and 2, respectively. Also, the transmission rate can be increased more than 2.6 and 2.7 times in the worst case for scenarios 1 and 2, respectively, if OPSA, instead of UPSA, is adopted. But when the transmit SNR is higher than 35 dB, C_{Unif}/C_{Optim} approaches one; both methods give similar results. We can also see that OPSA is more suitable for the best case of scenario 2 and for the worst case of scenario 1.

V. Conclusions

In this paper, we have presented a study of the capacity of an UWB channel for neural recording systems. Uniform and optimal capacities as well as the ratio of uniform capacity over optimal capacity were presented. The results are useful for the design of neural recording system in biomedical applications. These results are based on realistic simulations and are the first on the optimal capacity of the UWB channel for neural recording systems. Our results show the following.

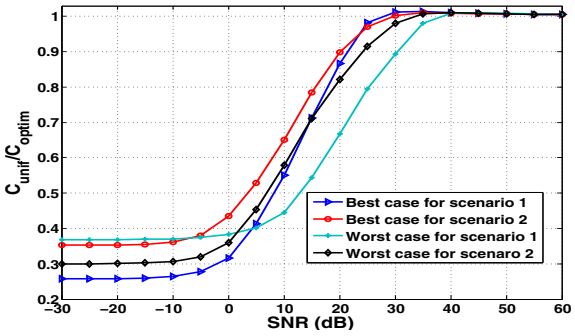

Fig. 8: Ratio of uniform capacity over optimal capacity.

- Differences in scenarios play an important role in the capacity. The capacities found in best case scenarios 1 and 2 are higher than it in the worst case scenarios 1 and 2.
- It is better to use the best case scenario 2 for this kind of biomedical systems.
- For best and worst cases (scenarios 1 and 2), when the transmit SNR is very low ($<$ 0 dB), using OPSA can increase the transmission rate by a factor between 2.3 and 3.2, depending on the scenario, compared to UPSA. When the transmit SNR is higher than 35 dB, both approaches, OPSA and UPSA, give similar results for best and worst cases.

References

[1] B. Gosselin, "Recent advances in neural recording microsystems," *Sensors*, vol. 11, pp. 4572–4597, 2011.

[2] B. Gosselin, A. Ayoub, J.-F. Roy, M. Sawan, F. Lepore, A. Chaudhuri, and D. Guitton, "A mixed-signal multichip neural recording interface with bandwidth reduction," *IEEE Transactions on Biomedical Circuits and Systems*, vol. 3, no. 3, pp. 129–141, 2009.

[3] N. Neihart and R. Harrison, "Micropower circuits for bidirectional wireless telemetry in neural recording applications," *IEEE Transactions on Biomedical Engineering*, vol. 52, no. 11, pp. 1950–1959, 2005.

[4] U.-M. Jow and M. Ghovanloo, "Optimization of data coils in a multiband wireless link for neuroprosthetic implantable devices," *IEEE Transactions on Biomedical Circuits and Systems*, vol. 4, no. 5, pp. 301–310, 2010.

[5] H. Bahrami, B. Gosselin, and L. A. Rusch, "Design of a miniaturized UWB antenna optimized for implantable neural recording systems," in *2012 IEEE 10th International New Circuits and Systems Conference (NEWCAS)*, 2012, pp. 309–312.

[6] H. Bahrami, B. Gosselin and L. A. Rusch, "Realistic modelling of the biological channel for the design of implantable wireless UWB communication systems," in *2012 Annual International Conference of the IEEE Engineering in Medicine and Biology Society (EMBC)*, 2012, pp. 6015–6018.

[7] F. Zheng, T. Kaiser, "On the Evaluation of Channel Capacity of UWB Indoor Wireless Systems," *IEEE Transactions on Signal Processing*, vol. 56, no. 12, pp. 6106–6113, Dec 2008.

[8] B. Sklar, *Digital Communications: Fundamentals and Applications*. Prentice Hall, 2nd edition, 2001.

[9] A. Drossos, V. Santomaa, and N. Kuster, "The dependence of electromagnetic energy absorption upon human head tissue composition in the frequency range of 300-3000 MHz," *IEEE Transactions on Microwave Theory and Techniques*, vol. 48, no. 11, pp. 1988–1995, 2000.

[10] S. Gabriel, R. W. Lau, and C. Gabriel, "The dielectric properties of biological tissues: III. Parametric models for the dielectric spectrum of tissues," *Physics in Medicine and Biology*, vol. 41, no. 11, pp. 2271–2293, 1996.